Food and Chemical Toxicology 125 (2019) 95–105

Contents lists available at ScienceDirect

Food and Chemical Toxicology

journal homepage: www.elsevier.com/locate/foodchemtox

Glucosamine induces increased musclin gene expression through endoplasmic reticulum stress-induced unfolding protein response signaling pathways in mouse skeletal muscle cells

Qian Guo[a,1], Hailong Hu[a,1], Ying Zhou[a,1], Yuheng Yan[a], Xiangjuan Wei[a], Xingpei Fan[a], Daqian Yang[a], Hongjuan He[a], Yuri Oh[b], Kun Chen[c], Qiong Wu[a], Chuanpeng Liu[a], Ning Gu[a,*]

[a] School of Life Science and Technology, Harbin Institute of Technology, Harbin, China
[b] Faculty of Education, Wakayama University, Wakayama, Japan
[c] The Joint Research Center of Guangzhou University and Keele University for Gene Interference and Application, School of Life Science, Guangzhou University, Guangzhou, China

ARTICLE INFO

Keywords:
Glucosamine
Musclin
Insulin resistance
Unfolding protein response
Skeletal muscle cells

ABSTRACT

Glucosamine (GlcN) is a dietary supplement that is widely used to promote joint health. Reports have demonstrated that oral GlcN adversely affects glucose metabolism. Here, we found that oral administration of GlcN induced insulin resistance (IR) and increased plasma glucose levels in mice. Musclin is a muscle-secreted cytokine that participates in the development and aggravation of diabetes. In this study, we found that increased expression of the musclin plays a pathogenic role in GlcN-induced IR in mice. Additional *in vivo* and *in vitro* studies showed that 4-PBA inhibited GlcN-induced endoplasmic reticulum (ER) stress and reduced musclin expression, indicating that ER stress might be closely linked to musclin expression. Moreover, the inhibition of musclin gene expression was also observed when sh-RNAs and small molecular compound inhibitors inhibited ER stress-induced PERK and IRE1-associated unfolding protein response (UPR) signaling pathways, and the CRISPR/Cas9 genome editing technology knockout the ATF6-associated UPR pathway in C2C12 myotubes cells. Silencing of the expression of musclin effectively relieved GlcN-affected phosphorylation of Akt, glucose intake and glycogen synthesis. These results suggest that GlcN increased musclin gene expression though UPR, and musclin represents an important mechanism underlying GlcN-induced IR in mice.

1. Introduction

Glucosamine (GlcN) is one of the most widely consumed dietary supplement in the world. Three common forms of GlcN supplements are currently available on the market: (1) glucosamine hydrochloride; (2) glucosamine sulfate; and (3) N-acetyl glucosamine (Anderson et al., 2005). GlcN and its acetylated derivative, N-acetyl glucosamine, are naturally occurring amino sugars found in the human body. They are important components of glycoproteins, proteoglycans, and glycosaminoglycans (Dalirfardouei et al., 2016). Scientific studies have supported the concept that GlcN has beneficial pharmacological effects in the alleviation of numerous diseases, including symptoms of osteoarthritis, temporomandibular joint disorders, and rheumatoid arthritis (Kong et al., 2009; Reginster et al., 2012). Recently, many studies have introduced novel biological and pharmacological applications of GlcN-based compounds, e.g. in the treatment of skin disorders, cancer, cardiovascular diseases, and kidney toxicity (Kong et al., 2009; Simon et al., 2011).

Such widespread consumption raises potential concerns about the safety and toxicity of these compounds. The most common unwanted adverse effects reported to date include mild gastrointestinal complaints such as heartburn, epigastric distress, diarrhea, nausea, and pyrosis (Kong et al., 2009; Simon et al., 2011). Numerous *in vitro* and animal studies have shown that GlcN induces insulin resistance (IR) in some organs (Anderson et al., 2005; Longo et al., 2016). IR is a key pathophysiological feature of type 2 diabetes mellitus (T2DM). In IR models, insulin secretion occurs at normal levels, but fails to effectively regulate plasma glucose levels (Liong and Lappas, 2016). According to

* Corresponding author. School of Life Science and Technology, Harbin Institute of Technology, Ning Gu, No. 92 West Da-zhi Street, Harbin, 150001, Heilongjiang, China.
E-mail address: guning@hit.edu.cn (N. Gu).
[1] These authors are thought to have equal contributions.

https://doi.org/10.1016/j.fct.2018.12.051
Received 3 August 2018; Received in revised form 24 December 2018; Accepted 28 December 2018
Available online 30 December 2018
0278-6915/

the literature, GlcN infusion in rats induces IR in response to glucose uptake in the whole body and at skeletal muscle levels (Anderson et al., 2005). Furthermore, GlcN induces IR *in vitro* in skeletal muscle by reducing insulin-induced glucose uptake (Longo et al., 2016). However, the mechanism by which GlcN induces IR is still unclear.

Musclin is a muscle-secreted cytokine that has received increased attention in recent years (Gu et al., 2015). Skeletal muscle, which is a major organ involved in energy expenditure, participates in the homeostasis of glucose metabolism. With respect to the action of insulin, skeletal muscle cells convert plasma glucose into myogenic glycogen (Plomgaard et al., 2007). Skeletal muscle also acts as an endocrine organ, producing bioactive molecules known as myokines (such as tumor necrosis factor-alpha [TNF-α] and interleukin-6 [IL-6]) (Pedersen and Febbraio, 2008). Among myokines, musclin is a newly discovered 130-amino acid peptide that was first reported by Nishizawa et al. (2004). In recent years, musclin has been regarded as a factor that contributes to the development and aggravation of diabetes (Chen et al., 2017; Gu et al., 2015). In T2DM, musclin gene expression is increased in skeletal muscle (Chen et al., 2017; Jeremic et al., 2017). In addition, administration of recombinant musclin protein has been shown to significantly reduce glucose uptake and glycogen synthesis in myocytes (Nishizawa et al., 2004). Although musclin represents a novel endogenous factor in animal models, the mechanism underlying its bioactivity and expression remains largely unknown. Further, it is not known whether musclin participates in the process of GlcN-induced IR.

In this study, we investigated the connection between GlcN and musclin gene expression. We treated mice with GlcN by oral administration and observed the effects of GlcN on musclin expression. In future studies, we aim to detect the molecular mechanism(s) underlying GlcN-induced increases in musclin expression in mice, as well as in mouse skeletal muscle C2C12 cells.

2. Materials and methods

2.1. Materials and reagents

GlcN (D-(+)-Glucosamine hydrochloride) and 4-phenylbutyric acid (4-PBA) were from Sigma-Aldrich (St Louis, Mo, USA), DMEM, FBS and BSA were from Invitrogen (Paisley, UK). Rodent diets were from Keao Co., Ltd. (Beijing, China). The glucose assay kit was from Wako Pure Chemical Industries, Ltd. (Osaka, Japan). The mouse insulin ELISA kit was from Shibayagi Co., Ltd. (Gunma, Japan). RNAiso, the PrimeScript RT reagent Kit and SYBR Premix Ex Taq II were from Takara (Tokyo, Japan). Antibodies were from Cell Signaling Technology (MA, USA). 2-(N-(7-nitrobenz-2-oxa-1,3-diazol-4-yl)-amino)-2-deoxyglucose (2NBDG) was from Invitrogen (MA, USA). Glycogen Assay kit was from Nanjing Jiancheng Bioengineering Institute (Nanjing, China).

2.2. Animals and treatments

All animal experiments were reviewed and approved by Ethics Research Committee of the School of Life Science and Technology of Harbin Institute of Technology, and carried out according to guidelines for the care and use of experimental animals approved by the Heilongjiang Province People's Congress (http://www.nicpbp.org.cn/sydw/CL0249/2730.html). Six-week-old CD-1 mice of 50 males (average body weight: 24.52 ± 0.58 g, average plasma glucose: 3.77 ± 0.19 mmoL/L) were obtained from Harbin Veterinary Research Institute (Harbin, China) and acclimated for 7 days after arrival at the study facility. Mice were housed in an animal room at controlled temperature (21–24 °C) and light cycle (12 h light/dark). Autoclaved water and rodent diets were provided ad libitum. Mice were randomly divided into five groups: 0 g/kg, 0.2 g/kg, 0.2 g/kg + 4-PBA, 0.5 g/kg, and 0.5 g/kg + 4-PBA groups. 0.2 g/kg body weight (b.w.) GlcN, 0.5 g/kg b.w. GlcN were given to mice of 0.2 g/kg, 0.5 g/kg groups by a syringe via the oral administration. 0.1 g/kg b.w. 4-PBA was given to 0.2 g/kg + 4-PBA and 50 g/kg + 4-PBA groups mice, in addition to the 0.2 or 0.5 g/kg b.w. GlcN. 0 g/kg group mice were given equal volume phosphate buffer saline (PBS).

2.3. Blood collection and analysis

Tail vein blood was collected every 2 weeks. Before the collection, mice were fasted for 16 h. At the end of week 26, after the fasted, blood was collected from heart. Tail vein blood and heart blood plasma glucose were measured using glucose assay kit. Heart blood plasma insulin was measured using mouse insulin ELISA kit. shRNA vectors were from GenePharma (Shanghai, China). Cell Signaling Technology (Danvers, MA, USA).

2.4. Oral glucose tolerance test (OGTT)

At week 20, mice were fasted for 16 h and then orally administered glucose (1.5 g/kg body weight). Blood was collected for plasma glucose and insulin measurement from the tail vein at 0, 30, 60, 120 min by each kits as above described.

2.5. Cells culture

Mouse C2C12 myoblasts were maintained in Dulbecco's modified Eagle's medium supplemented with 10% fetal bovine serum, penicillin (50 units/mL), and streptomycin (50 mg/mL). When cells reached confluence, the medium was transferred to the differentiation medium containing Dulbecco's modified Eagle's medium and 2% horse serum defined as the differentiation medium, which was changed every other day. After ten additional days, the differentiated C2C12 cells had fused into myotubes.

GlcN was added to DMEM to final concentration of 7.5 and 15 mmoL/L (mM). The differentiated C2C12 cells were then treated in each condition for specified time.

2.6. Cell transfection

The shRNA-mediated knockdown of PERK, IRE1 and musclin was perfomed by shRNA vector containing an inverted repeat of the interference sequence. These interference sequences of the shRNA used in the study were as follows: shRNA-PERK (5′-GCAGGTCCTTGGTAATCA TCA-3′); shRNA-IRE1 (5′-GGAATTACTGGCTTCTCAT-3′); shRNA-musclin (5′-GAATTGTTGTAAACTTCAACT-3′). In addition, the scrambled sequence as a shRNA-control was 5′-GTTCTCCGAACGTGTCACGT-3'. C2C12 myotubes differentiated for 10 days were transfected with shRNA plasmids using electro porator NEPA21 according to the manufacturer's procedure (NEPA Gene, Chiba, Japan). Once finished, the cells were immediately transferred to the fresh media with 2% horse serum.

2.7. Measurement of glucose uptake and glycogen synthesis

After 2 h incubation in no glucose DMEM, myotubes were incubated with or without 1 μM insulin for another 1 h. For glucose uptake measurement, myotubes were transferred to fresh no glucose DMEM medium supplemented with 80 μM fluorescent deoxyglucose 2NBDG for 30 min. After three times washed by PBS, myotubes were lysed by 0.5% TritonX-100 and the fluorescence intensity was recorded using a fluorescence microplate reader (Hitachi) at excitation and emission wavelengths of 485 and 538 nm, respectively. For glycogen synthesis measurement, myotubes were hydrolyzed with NaOH and H_2O_2, and the total amount of glycogen was measured by using the Glycogen Assay kit. The absorbance was recorded using a microplate reader (Tecan) at 630 nm.

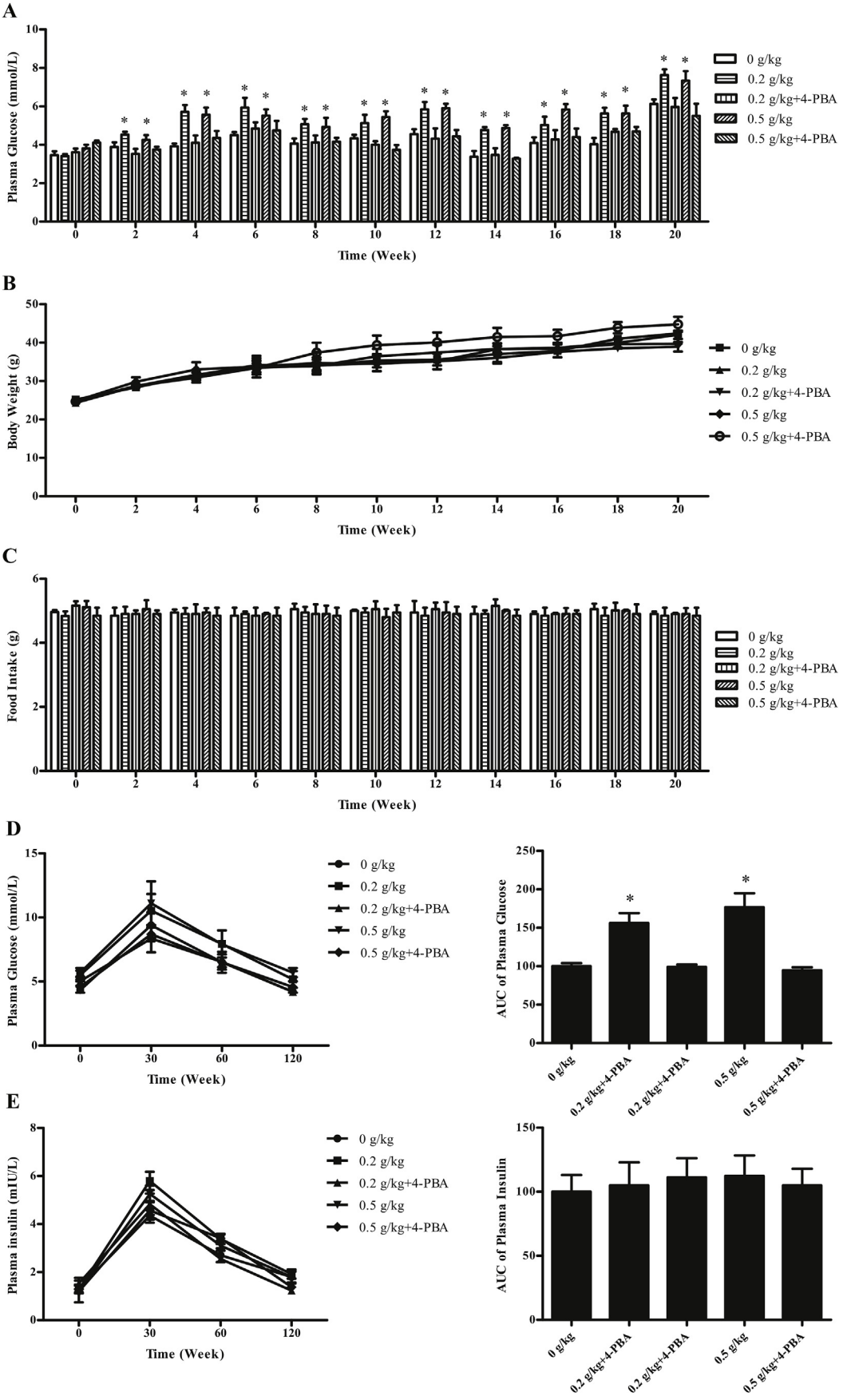

(caption on next page)

Fig. 1. Oral administration of GlcN induce insulin resistance, and thus increased plasma glucose in mice. (A) The plasma glucose levels of mice tail veins. (B) Body weights. (C) Food intakes. (D) Time course of changes and area under the curve (AUC) in plasma glucose levels during the OGTT. (E) Time course of changes and area under the curve (AUC) in plasma insulin levels during the OGTT. Mice were orally administered with GlcN everyday (0.2 and 0.5 g/kg b.w per day, 7 days per weeks for 20 weeks). Plasma glucose levels, body weights and food intakes were measured every two weeks. In week 20, mice were fasted for 16 h and then orally administered glucose (1.5 g/kg b.w.). Plasma glucose and insulin levels were measured at 0, 30, 60 and 120 min $^{*}P < 0.05$ vs. 0 g/kg b.w. group. Results are mean ± SE (n = 10).

2.8. CRISPR-cas9 and generation of knockout cell lines

CRISPR/Cas9 genome editing technology was performed by using the pX330-U6-Chimeric_BB-CBh-hSpCas9 plasmid to knockout ATF6. Short guide RNAs (sg RNAs) against ATF6 were designed using the http://crispr.dbcls.jp/platform (Naito et al., 2015). Briefly, 0.1 pmoL/μL sg RNA pairs (5-TTTAGTCCGGTTCTTCCTCAT-3 and 5-ATGAGGAA GAACCGGACTAAA-3) were introduced to the pX330-U6-Chimeric_BB-CBh-hSpCas9 plasmid through digestion/ligation cycles using BbsI and ligation high Ver.2 (TOYOBO, Japan). The recombinant plasmids were then transfected into C2C12 cells. After 24 h, C2C12 cells were seeded into 96-well plates. After approximately 14 days, surviving single cell clones were selected and resuspended in a 12-well plate containing 1 mL of medium. Single clones were analyzed by western blotting and subsequently further characterized. The knockout cell clones were stored in liquid nitrogen using freezing medium.

2.9. Quantitative real-time polymerase chain reaction (RT-PCR)

Total RNA from mice back-leg skeletal muscle tissues or C2C12 myotubes was prepared using RNAiso. First-strand cDNA was synthesized from total RNA using PrimeScript RT reagent Kit. To quantify mRNA expression, RT-PCR was performed with the ABI7000 using the SYBR Premix Ex Taq II according to the manufacturer's protocol. Respective primer sets (forward and reverse) were as follows: musclin, 5-TGTGGACTTAGCATCACAGG-3 and 5-AGCTGAGAGTCTGTCAAGG-3; GRP78, 5-CGTATCCCCTGCGTCTTGTC-3 and 5-CAGCAGCCTCCGGCT CTA-3; CHOP, 5-GGGAAACAGCGCATGAAGGA-3 and 5-GCGTGATGG TGCTGGGTACA-3; PERK, 5-AGTCCCTGCTC GAATCTTCCT-3 and 5-TCCCAAGGCAGAACAGATATACC-3; IRE1, 5-AGTATTCCACCAGCCTC TATGC-3 and 5-CACACACTCTCCTTTGT-3; ATF6, 5-TGGGCAGGACTA TGAAGTAATG-3 and 5-CAACGACTCAGGGATGGTGCTG-3; XBP1-s, 5-TGAGAACCAGGAGTTAAGAA-3 and 5-CCTGCACCTGCTGCGGAC-3; XBP1-u, 5-TGAGAACCAGGAGTTAAGAACACGC-3 and 5-CACATAGTC TGAGTGCTGCGG-3; 36B4, 5-GTAGTCAGTCTCCACAGACAAAG-3 and 5-CCGTGTGAGGTCACAGTACC-3; Quantification of gene expression was determined by comparative quantity, using 36B4 gene expression as inner control.

2.10. Western blot

0.3 g of skeletal muscle tissues or C2C12 myotubes was resuspended in RIPA lysis buffer. Lysates were centrifuged for 15 min at 4 °C and protein contents of the supernatant were determined using DC protein assay reagents package (Bio-Rad Laboratories, CA, USA). Aliquots of the proteins were separated by 10% sodium dodecyl sulfate-polyacrylamide gel electrophoresis, and transferred to PVDF membranes purchased from Bio-Rad Laboratories (CA, USA). For western blots, membranes were incubated with antibodies. Antibodies against phosphorylation-eIF2α, GRP78, CHOP, ATF6, XBP1, PERK, IRE1, phosphorylation-Akt, Akt, β-actin. Bands were visualized using an ECL plus western blotting detection system (GE Healthcare, UK).

2.11. Statistical analysis

Statistical differences between groups were evaluated by Student's t-test and were considered significant when $p < 0.05$.

3. Results

3.1. Oral administration of GlcN induces insulin resistance in mice

The mean fasting plasma glucose levels of the five groups of mice were similar prior to oral administration of GlcN. Blood was drawn from the tail vein of mice during the oral administration phase. Plasma glucose levels were measured and found to have increased from week 2 in both the 0.2 and 0.5 g/kg b.w. groups. Meanwhile, 4-phenylbutyric acid (4-PBA) treatment effectively reduced the GlcN-induced increase in plasma glucose in mice (Fig. 1A). Body weight and food intake were measured during the same period, and no significant differences were found between the five groups (Fig. 1B and C).

The measurement of mice plasma glucose levels from tail vein blood was performed until week 20. After it was determined that the increase in plasma glucose was not an isolated phenomenon, an oral glucose tolerance test (OGTT) was administered in order to examine glucose-dependent insulin secretion in mice at week 20 after oral administration of GlcN. There was a significant increase in plasma glucose levels, but no differences in plasma insulin levels at 30, 60, and 120 min after oral glucose administration in the 0.2 and 0.5 g/kg b.w. groups when compared with the 0 g/kg b.w. group (Fig. 1 D and E). The area under the curve (AUC) for plasma glucose was higher in the 0.2 and 0.5 g/kg b.w. groups than in the 0 g/kg b.w. group; however, there was no significant difference between the 0.2 and 0.5 g/kg b.w. groups (Fig. 1D). There was no significant difference in the AUC of plasma insulin between the five groups (Fig. 1E). Further, 4-PBA was shown to inhibit the effects of GlcN on plasma glucose (Fig. 1D and E).

The results indicate that oral administration of GlcN did not affect insulin secretion, but did induce IR, thereby inducing a significant increase in plasma glucose levels in mice.

3.2. Oral administration of GlcN induced endoplasmic reticulum stress and increased musclin gene expression in mice

At week 20, mice were fasted for 16 h and then euthanized. Mice skeletal muscles were collected to analyze levels of endoplasmic reticulum (ER) stress. Quantitative reverse transcription polymerase chain reaction (RT-qPCR) results showed that the expression of CCAAT enhancer binding protein (C/EBP) homologous protein (CHOP) and glucose-regulated protein (GRP)78 genes as well as the mRNA ratio of spliced xeroderma pigmentosa (XPB)1/total XPB1 (XBP1-s/XBP1-t) significantly increased in the 0.2 and 0.5 g/kg b.w. groups. Activating transcription factor (ATF)4 gene expression levels significantly increased in the 0.5 g/kg b.w. group (Fig. 2A). Agarose gel electrophoresis results verified changes in the mRNA ratio of XBP1-s/XBP1-t (Fig. 2B and C). Western blot results showed that, in the 0.2 and 0.5 g/kg b.w. groups, GlcN caused an increase in the protein expression of phospho-Eif2α (p-Eif2α), GRP78, and CHOP, and protein ratios of XBP1-s/XBP1-t and 50 KD/90 KD ATF6 (Fig. 2D and E). As shown in Fig. 2A–E, 4-PBA inhibited all of the above described effects of GlcN on ER stress markers.

The 0.2 and 0.5 g/kg b.w. GlcN groups also showed a significant increase in musclin gene and protein expression. The effects of GlcN on musclin gene and protein expression in mice were effectively inhibited by 4-PBA (Fig. 2A and C).

These results suggest that GlcN activated the PERK, IRE1, and ATF6 pathways, and thus induced ER stress, and GlcN promoted musclin

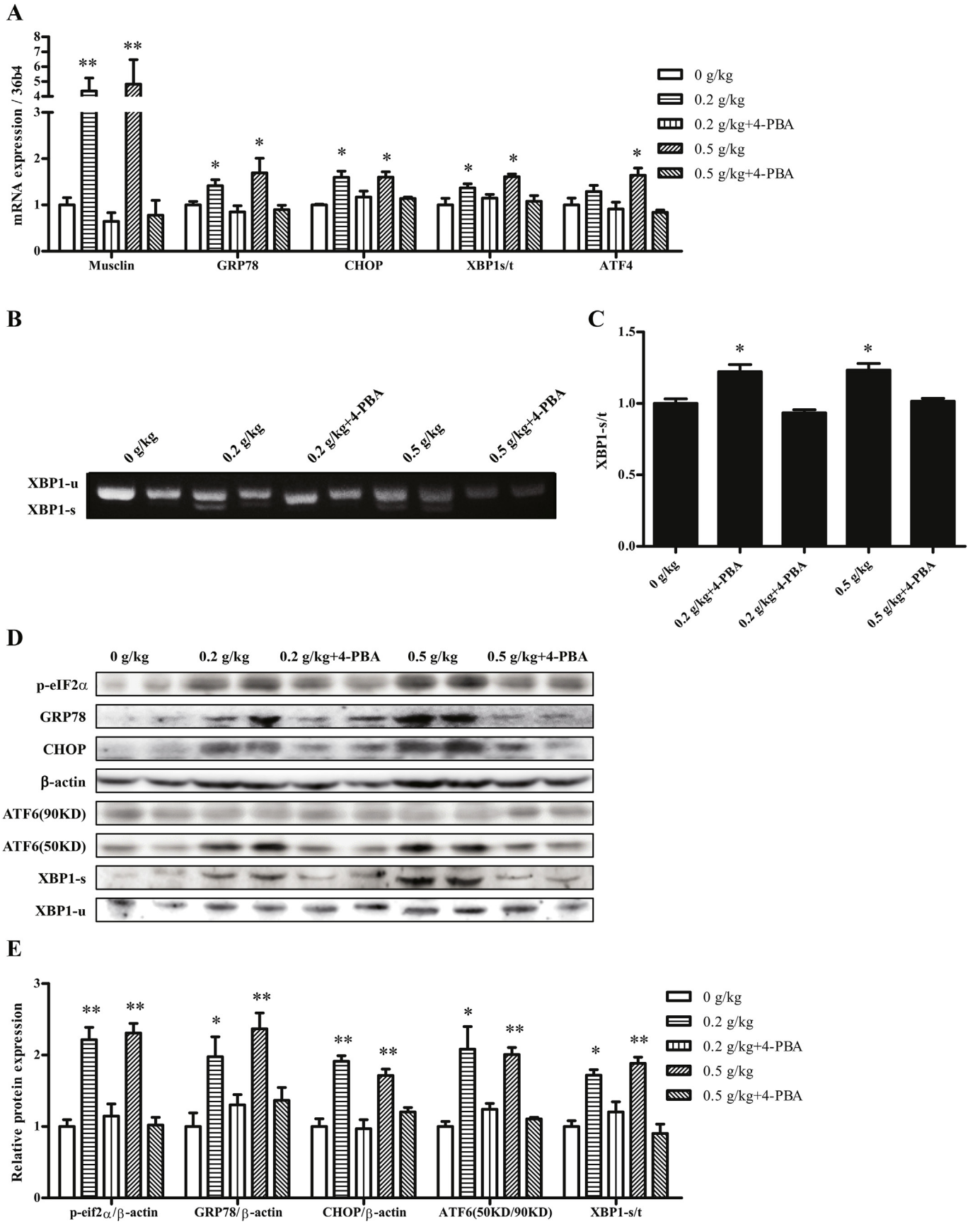

Fig. 2. Oral administration of GlcN induced ER stress and increased musclin gene expression in mice. (A) The mRNA expressions. (B) AGE of XBP1-s and XBP1-t. (C) The mRNA ratio of XBP1-s/t. (D). The protein expressions of ER stress markers. (E). The protein ratios of p-eif2α/β-actin, GRP78/β-actin, CHOP/β-actin, 50 KD ATF6/90 KD ATF6, XBP1-s/t. Each tissues were collected in week 20. $^{*}P < 0.05$, $^{**}P < 0.01$ vs. 0 g/kg b.w. group. Results are mean ± SE (n = 10).

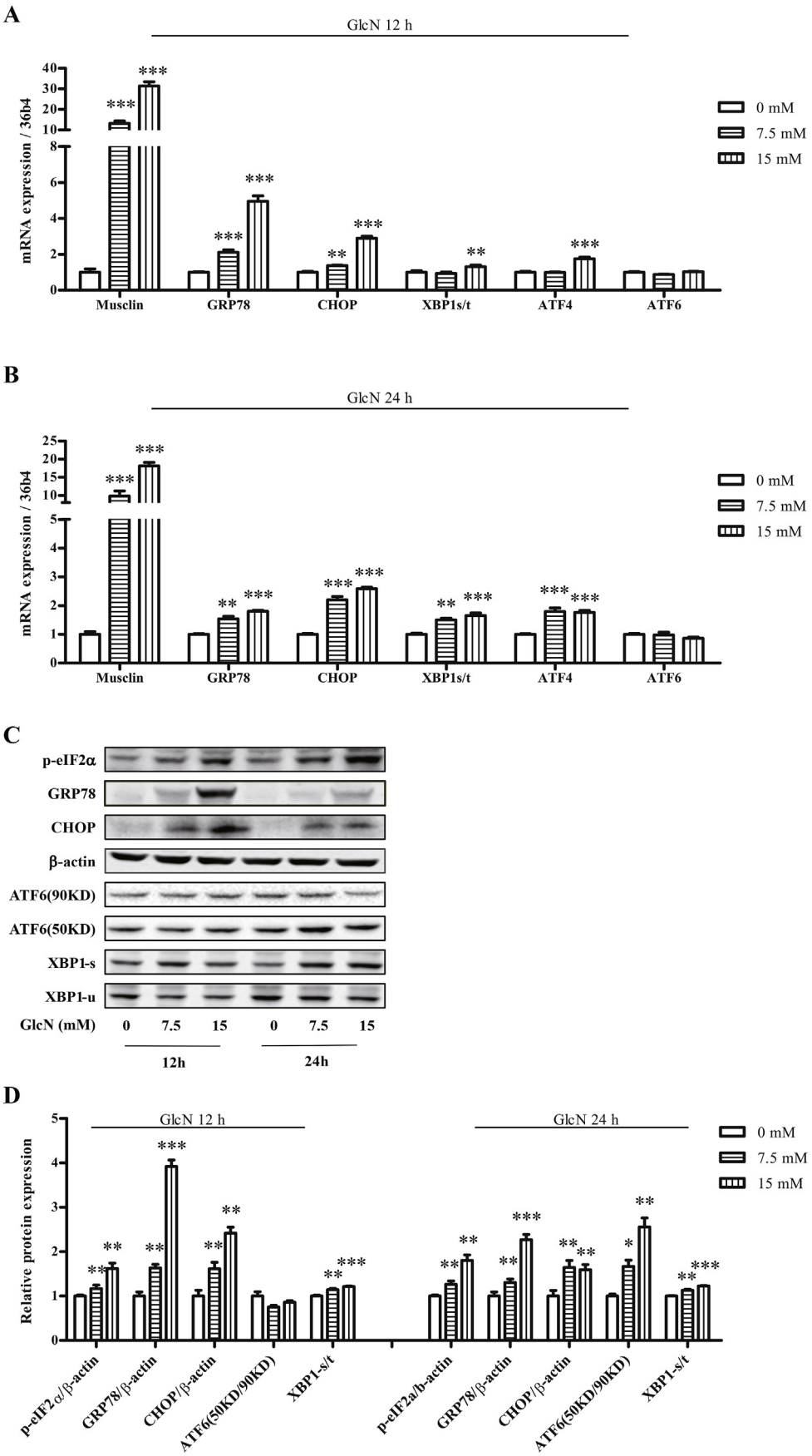

Fig. 3. GlcN induced ER stress and increased musclin gene expression in C2C12 myotubes. (A) The mRNA expressions of C2C12 myotubes after treated with 7.5 and 15 mM GlcN for 12 h from the seventh day of differentiation. (B) The mRNA expressions of C2C12 myotubes after treated with 7.5 and 15 mM GlcN for 24 h from the seventh day of differentiation. (C) The protein expressions of C2C12 myotubes after treated with 7.5 and 15 mM GlcN for 12 h or 24 h from the seventh day of differentiation. (D) The protein ratios of p-eif2α/β-actin, GRP78/β-actin, CHOP/β-actin, 50 KD ATF6/90 KD ATF6, XBP1-s/t. $^{*}P < 0.05$, $^{**}P < 0.01$, $^{***}P < 0.001$ vs. 0 mM group. Results are mean ± SE (n = 10).

expression in mice. Alleviation of ER stress by 4-PBA effectively inhibited the GlcN-induced increase in musclin expression.

3.3. GlcN induced ER stress and increased musclin gene expression in C2C12 myotubes

C2C12 myotubes were induced into a differentiated state, and gene and protein expression was tested at 12 and 24 h after treatment with 7.5 and 15 mM GlcN. GRP78, CHOP, and musclin gene expression significantly increased at 12 h and then leveled off at high levels at 24 h in both the 7.5 and 15 mM GlcN groups. At 12 h, the mRNA ratio of XBP1-s/XBP1-t and ATF4 gene expression significantly increased in the 15 mM group. However, at 24 h, the mRNA ratio of XBP1-s/XBP1-t and ATF4 gene expression significantly increased in both the 7.5 and 15 mM groups (Fig. 3A and B). Western blotting results showed that eukaryotic translation factor p-eIF2α, GRP78, and CHOP protein expression, and the protein ratio of XBP1-s/XBP1-t significantly increased at 12 h and then leveled off at high levels at 24 h in both the 7.5 and 15 mM groups (Fig. 3C and D). GlcN (at 7.5 and 15 mM) did not affect the protein ratio of 50KD ATF6/90 KD ATF6 at 12 h, but induced an increase in the protein ratio of 50KD ATF6/90 KD ATF6 at 24 h (Fig. 3C and D).

These results suggest that GlcN activated the PERK, IRE1, and ATF6 pathways, and thus induced ER stress, and GlcN promoted musclin expression in C2C12 myotubes.

3.4. Inhibition of PERK pathway inhibited effects of GlcN on musclin

To examine the correlation between the GlcN-induced ER stress and increase in musclin gene expression, we inhibited the protein kinase RNA-like endoplasmic reticulum kinase (PERK) pathway by treating C2C12 myotube cells with sh-PERK and 5 μM GSK2656157, which is a PERK pathway inhibitor. We then tested PERK pathway-related protein and gene expression at 24 h after 7.5 mM GlcN treatment. Results showed that sh-PERK effectively inhibited GlcN-increased protein expressions of PERK and p-eIF2α and mRNA expression of PERK, ATF4, and CHOP. Further, sh-PERK effectively inhibited GlcN-increased mRNA expression of musclin (Fig. 4 A and B). GSK2656157 also effectively inhibited GlcN-induced increase in p-eIF2α protein expression and ATF4 mRNA expression. In addition, GSK2656157 effectively inhibited the GlcN-induced increase in musclin mRNA expression (Fig. 4 C and D).

Therefore, inhibition of the PERK pathway inhibited the GlcN-induced increase in musclin gene expression, indicating that this pathway plays a role in the GlcN-induced increase in musclin expression.

3.5. Inhibition of IRE1 pathway abrogated effects of GlcN on musclin

We inhibited the IRE1 pathway by treating myotubes with sh-IRE1 and 30 μM 4-methyl umbelliferone 8-carbaldehyde (4μ8c), which is an IRE1 pathway inhibitor. Then, we tested IRE1 pathway-related protein and gene expression at 24 h after treatment with 7.5 mM GlcN. Results showed that sh-IRE1 effectively inhibited the GlcN-induced increase in IRE1 protein expression and protein ratio of XBP1-s/XBP1-t, IRE1 mRNA expression, and mRNA ratio of XBP1-s/XBP1-t. Further, sh-IRE1 effectively inhibited the GlcN-induced increase in mRNA musclin expression (Fig. 5 A and B). Additionally, 4μ8c effectively inhibited the GlcN-induced increase in the protein and mRNA ratio of XBP1-s/XBP1-t. GSK2656157 effectively inhibited the GlcN-induced increase in musclin mRNA expression (Fig. 5 C and D).

Therefore, inhibition of IRE1 pathway suppresses the GlcN-induced increase in musclin gene expression, indicating that this pathway participates in the GlcN-induced increase in musclin expression.

3.6. Inhibition of ATF6 pathway suppressed the effects of GlcN on musclin

We inhibited the myotube ATF6 pathway using the Clustered Regularly Interspaced Short Palindromic Repeats (CRISPR/Cas9) genome editing technology (Fig. 6 A); Cas9-ATF6 cell clones were selected for further analysis 24 h after treatment with 7.5 mM GlcN. Results showed that levels of cell differentiation in Cas9-ATF6 myotube

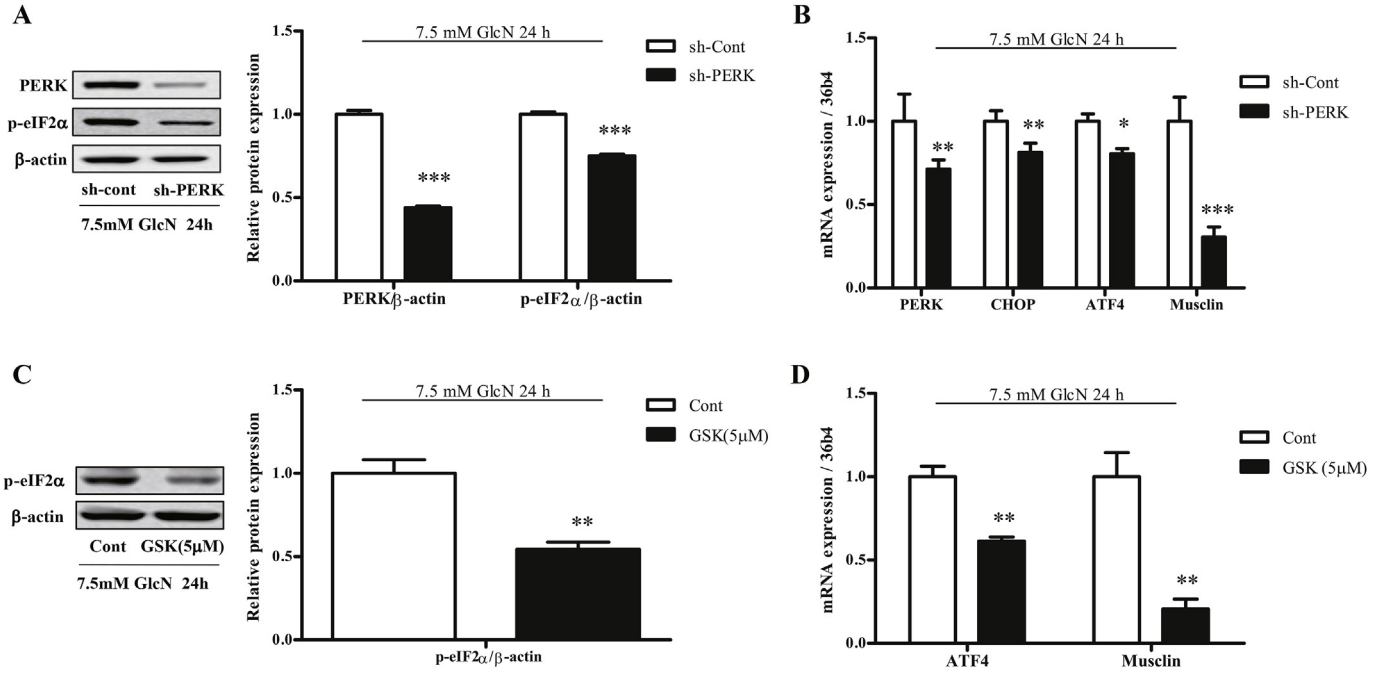

Fig. 4. Inhibition of PERK pathway inhibited effects of GlcN on Musclin. (A) The protein expressions of sh-control or sh-PERK treated C2C12 myotubes after treated with 7.5 mM GlcN for 24 h, and protein ratios of PERK/β-actin and p-eif2α/β-actin. (B) The mRNA expressions of sh-control or sh-PERK treated C2C12 myotubes after treated with 7.5 mM GlcN for 24 h. (C) The protein expressions of control or 5 μM GSK treated C2C12 myotubes after treated with 7.5 mM GlcN for 24 h, and protein ratio of p-eif2α/β-actin. (D) The mRNA expressions of control or 5 μM GSK treated C2C12 myotubes after treated with 7.5 mM GlcN for 24 h. The cells were manually counted from 4 independent experiments performed. $^{*}P < 0.05$, $^{**}P < 0.01$, $^{***}P < 0.001$ vs. sh-control or control group. Results are mean ± SE.

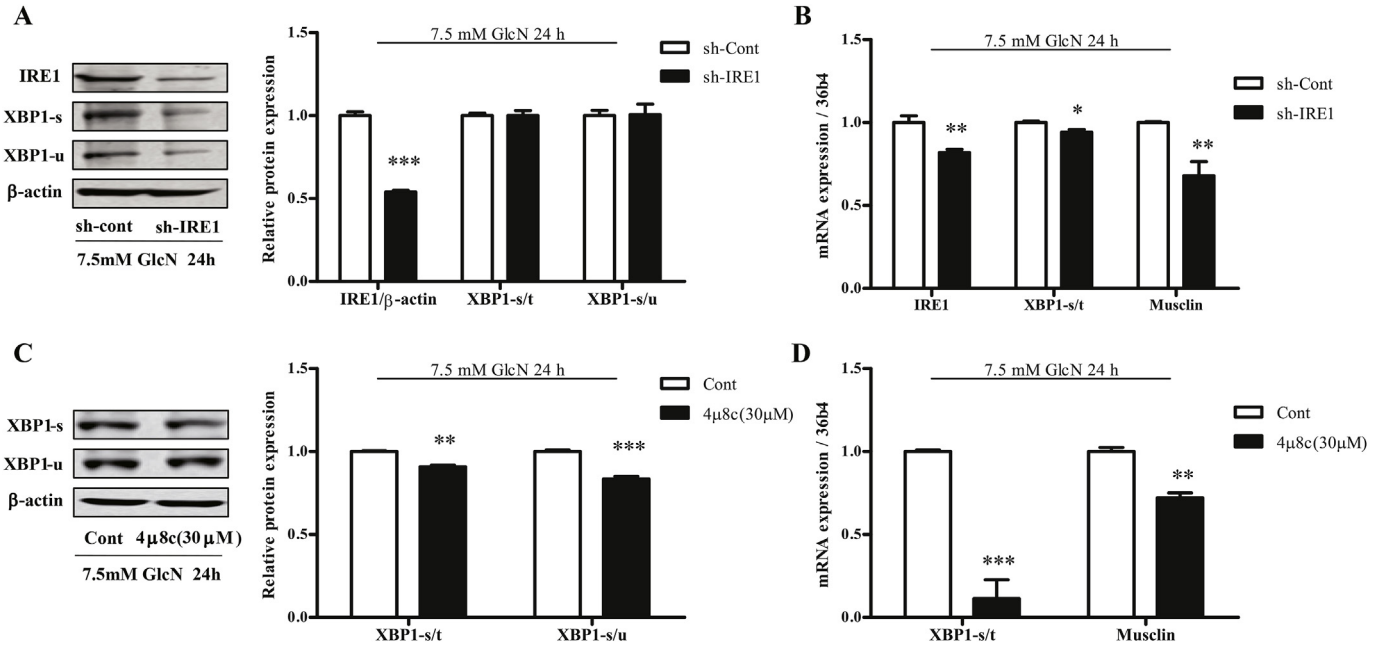

Fig. 5. Inhibition of IRE1 pathway inhibited effects of GlcN on Musclin. (A) The protein expressions of sh-control or sh-IRE1 treated C2C12 myotubes after treated with 7.5 mM GlcN for 24 h, and protein ratios of IRE1/β-actin, XBP1-s/t and XBP1-s/u. (B) The mRNA expressions of sh-control or sh-IRE1 treated C2C12 myotubes after treated with 7.5 mM GlcN for 24 h. (C) The protein expressions of control or 30 μM 4μ8c treated C2C12 myotubes after treated with 7.5 mM GlcN for 24 h, and protein ratio of p-eif2α/β-actin. (D) The mRNA expressions of control or 30 μM 4μ8c treated C2C12 myotubes after treated with 7.5 mM GlcN for 24 h. The cells were manually counted from 4 independent experiments performed. $^{*}P < 0.05$, $^{**}P < 0.01$, $^{***}P < 0.001$ vs. sh-control or control group. Results are mean ± SE.

cells were similar to those in wild-type (WT) C2C12 myotube cells (Fig. 6 B); however, the protein expression of ATF6 could not be observed in Cas9-ATF6 myotube cells (Fig. 6 C). Further, musclin mRNA expression was significantly reduced in GlcN-treated Cas9-ATF6 myotube cells (Fig. 6 D).

Therefore, inhibition of ATF6 pathway abrogates the effects of GlcN on musclin, indicating that this pathway participates in the GlcN-induced increase in musclin expression.

3.7. Silencing of musclin suppressed the effects of GlcN on insulin resistance

We silenced the musclin gene expression in C2C12 myotube cells by using sh-RNA, the result showed that sh-RNA effectively inhibited the musclin gene expression (Fig. 7A). Then we tested the insulin sensitivity by measured phosphorylation of Akt. Results showed that GlcN significantly reduced phosphorylation of Akt, and silencing of musclin effectively relieved the effects of GlcN on Akt (Fig. 7B and C). Meanwhile, we tested the glucose intake. From the fluorescence microscope,

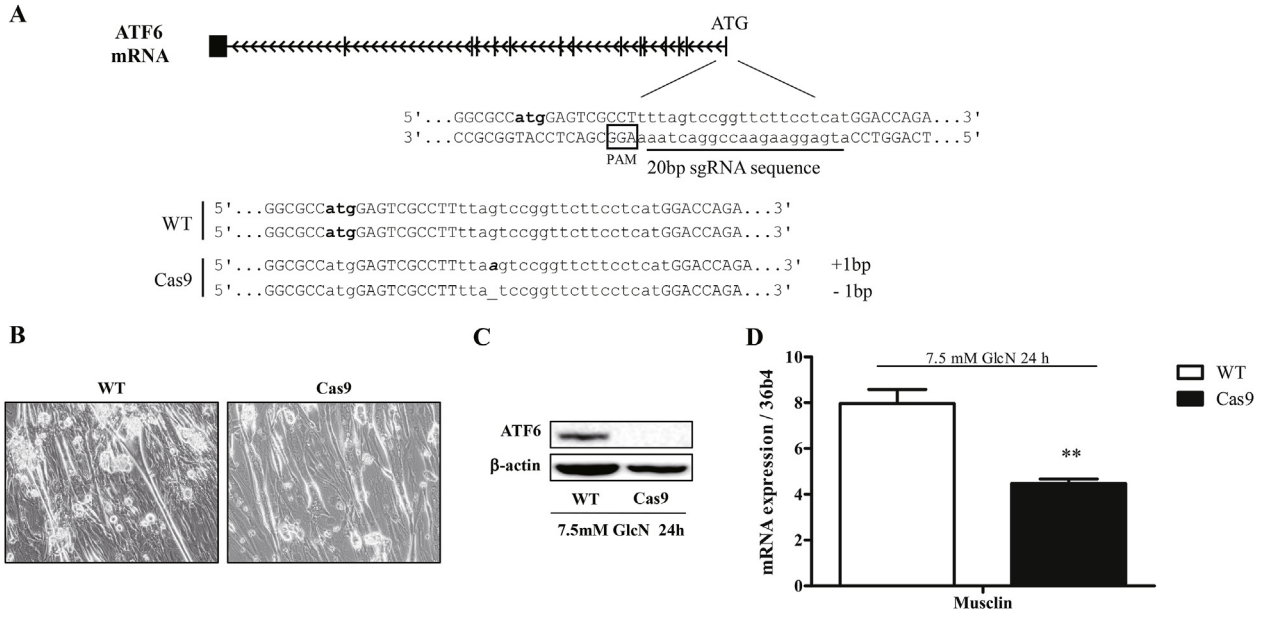

Fig. 6. Inhibition of ATF6 pathway inhibited effects of GlcN on Musclin. (A) CRISPR/Cas9-induced mutants in ATF6 of C2C12 myotubes. (B) Cell morphology of C2C12 myotubes. (C) The protein expressions of ATF6 in WT or CRISPR/Cas9-induced mutants C2C12 myotubes after treated with 7.5 mM GlcN for 24 h, and protein ratios of ATF6/β-actin. (D) The protein expressions of musclin in WT or CRISPR/Cas9-induced mutants C2C12 myotubes after treated with 7.5 mM GlcN for 24 h. The cells were manually counted from 4 independent experiments performed. $^{**}P < 0.01$ vs. WT group. Results are mean ± SE.

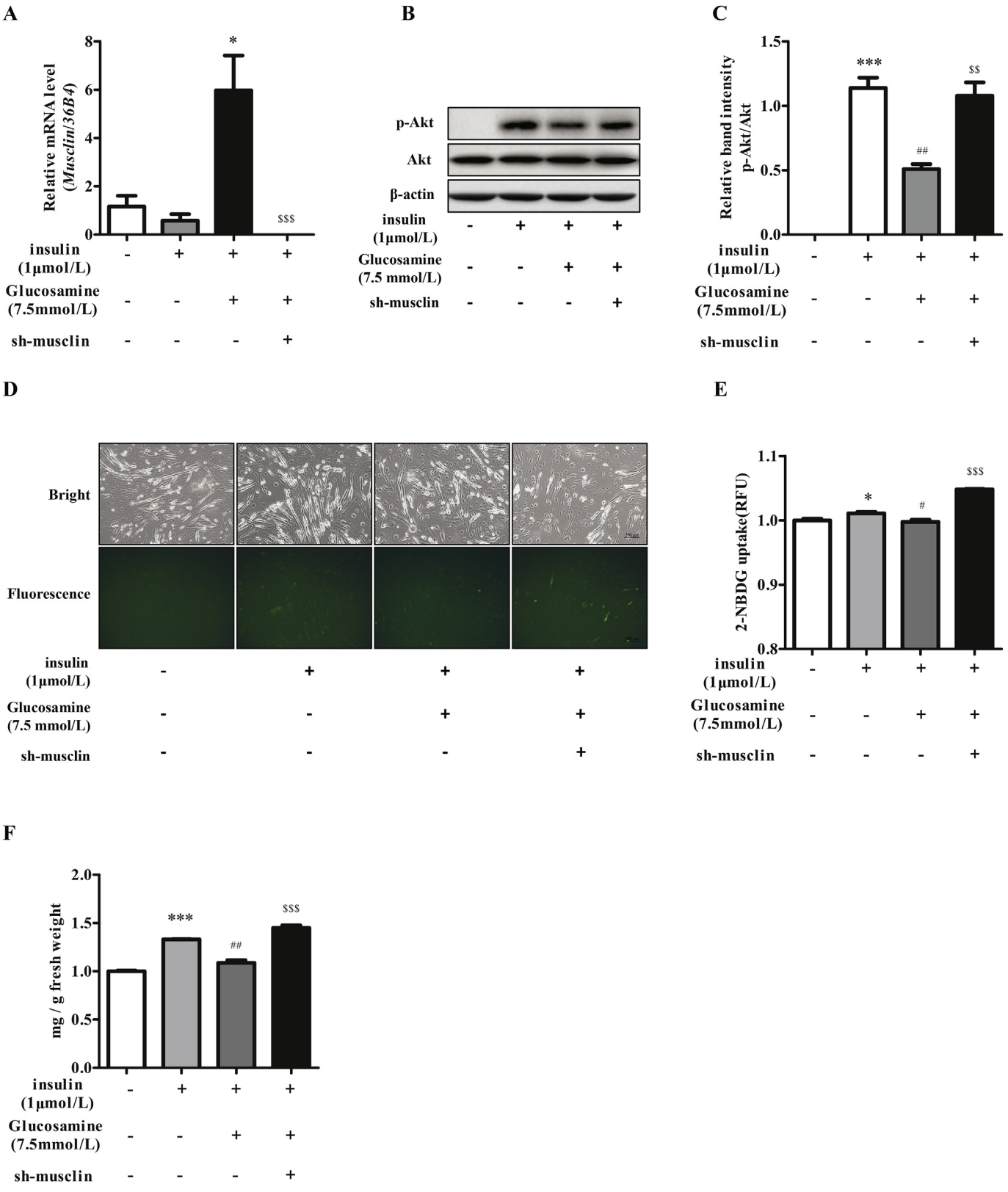

Fig. 7. Silencing of musclin suppressed the effects of GlcN on insulin resistance. (A) The gene expression of musclin in C2C12 myotube cells after treated with insulin, GlcN or sh-musclin. (B) The phosphorylation of Akt in C2C12 myotube cells after treated with insulin, GlcN or sh-musclin. (C) The protein ratios of p-Akt/Akt. (D) The 2-NBDG fluorescence in C2C12 myotube cells observed by the fluorescence microscope. (E) The 2-NBDG fluorescence in C2C12 myotube cells measured by fluorescence microplate reader. (F) The glycogen synthesis in C2C12 myotube cells. The cells were manually counted from 4 independent experiments performed. $^{*}P < 0.05$, $^{***}P < 0.001$ vs. control group. $\#P < 0.05$, $\#\#P < 0.01$, $\#\#\#P < 0.001$ vs. insulin treatment group. \$\$\$ $P < 0.001$ vs. insulin and GlcN treatment group. Results are mean ± SE.

compared with blank control, insulin treatment increased glucose intake. GlcN treatment reduced glucose intake. Silencing of musclin relieved GlcN-reduced glucose intake (Fig. 7D). The fluorescence microplate reader result also showed that the silencing of musclin relieved GlcN-reduced glucose intake (Fig. 7E). Then we tested the glycogen synthesis. The result showed that GlcN reduced glycogen synthesis and silencing of musclin effectively relieved GlcN-reduced glycogen synthesis (Fig. 7F).

4. Discussion

GlcN is a widely used dietary supplement that has been described as efficacious for individuals with osteoarthritis, especially for those with knee-related arthritis (Dalirfardouei et al., 2016; Reginster et al., 2012). GlcN is typically used at a dose of 1500 mg/day (21 mg/kg b.w.); however, higher doses of 3200 mg/day (45 mg/kg b.w.) have been used in some clinical trials (Dalirfardouei et al., 2016; Simon et al., 2011). Concerns have been raised about its safety and toxicity (Kong et al., 2009; Simon et al., 2011). Studies reported that GlcN consumption may worsen glucose tolerance and induce IR (Anderson et al., 2005; Longo et al., 2016). Taking into consideration the differences between the life spans of mice and humans, we treated mice with 0.2 and 0.5 g/kg b.w. GlcN by oral administration; these doses correspond to 10 times the daily recommended intake in human. In this study, the observed increase in plasma glucose levels and the IR were caused by GlcN treatment, at both 0.2 and 0.5 g/kg b.w., and not food intake or body weight.

Musclin, a myokine that is predominantly expressed in skeletal muscle, exerts potent effects on glucose intake and is regarded as an important mediator of complex metabolic processes (Pedersen and Febbraio, 2008; Plomgaard et al., 2007). Previous studies by Nishizawa et al. suggested that musclin mRNA expression is increased in the gastrocnemius muscle of obese KKAy mice and obese db/db mice (Nishizawa et al., 2004). *In vitro* studies have demonstrated that musclin significantly inhibited insulin-stimulated 2-deoxy-D-[1–3H]-glucose (2-DG) uptake and glycogen synthesis (Chen et al., 2017; Nishizawa et al., 2004). The present results supported the common view that GlcN is capable of inducing IR; however, a specific mechanism linking GlcN and musclin has not yet been established. In our study, we demonstrated, for the first time, a significant increase of the expression of musclin gene concomitant with GlcN-induced IR in mice. Accordingly, we speculated that an increase in musclin gene expression plays a pathogenic role in the GlcN-induced IR in mice. However, mechanisms underlying the elevation in musclin expression in GlcN-treated mice are not fully understood.

Many investigators have suggested that GlcN toxicity may contribute to ER stress (Gu et al., 2015; van der Harg et al., 2017). The ER forms a major compartment in eukaryotic cells and is responsible for maintaining protein homeostasis (Liu et al., 2017; Longo et al., 2016). Under conditions of cellular stress leading to ER function impairment, proteins become incapable of folding properly and accumulate in ER lumen (Liong and Lappas, 2016; Takahashi et al., 2017). As a result, the ER has evolved a cell protective mechanism, namely ER stress, which is collectively termed the unfolded protein response (UPR) (Liu et al., 2017). ER stress plays an important role in several human diseases, including T2DM (Bohnert et al., 2018; van der Harg et al., 2017). The chemical chaperone 4-PBA is known to attenuate ER stress (Kim et al., 2013; Su et al., 2013). In this study, 4-PBA inhibited GlcN-induced IR; further, 4-PBA inhibited the GlcN-induced increase in musclin gene expression, indicating that elevation of musclin expression is closely related to GlcN-induced ER stress.

Generally, UPR activation is dependent on three ER stress upstream sensor proteins: (1) PERK; (2) IRE1; and (3) ATF6, which bind to an ER stress indicator (binding immunoglobulin protein/GRP78), to restore ER homeostasis (Su et al., 2013; Wu et al., 2018). When ER stress occurs, the PERK, IRE1, and ATF6 pathways coordinate multiple genes, including anti-oxidant response-, inflammatory-, and foldase-related genes (Bohnert et al., 2018; Takahashi et al., 2017). Activated PERK phosphorylates eIF2α, leading to an increase in sensitivity to ER stress and elevated rates of cell death (Rozpedek et al., 2016; Park et al., 2014). ATF4 translation is activated following PERK-mediated phosphorylation of eIF2α; this is termed selective translation (Malhi and Kaufman, 2011; Park et al., 2014). Activated IRE1 cleaves XBP1 pre-mRNA encoding for XBP1u in the cytoplasm. This cytoplasmic splicing results in a new protein, termed XBP1s, with transcriptional activity (Cubillos-Ruiz et al., 2017; Liu et al., 2017). ATF6, a 670 amino acid, ER-transmembrane protein, is triggered by ER protein misfolding, and the N-terminal 50-kDa fragment of ATF6, which is about 400 amino acids in length, translocates to the nucleus to induce the expression of ER stress response genes (Bettigole and Glimcher, 2015; Biazi et al., 2017). When ER stress becomes severe and prolonged, cell death pathways, such as those associated with transcription factor CHOP, caspase 9, and c-Jun NH_2-terminal kinase, are activated (Harrison et al., 2018; Wu et al., 2018). By measuring the gene and protein expressions of UPR markers, this study demonstrate that GlcN activated the PERK, IRE1, and ATF6 pathways in both mice and C2C12 myotube cells. Therefore, changes in musclin expression are likely mediated by these three pathways.

Few investigations have addressed the correlation between ER stress and musclin gene expression. In this study, to determine whether the PERK, IRE1, and/or ATF6 pathways are involved in musclin gene expression induced by GlcN, these three pathways were verified in GlcN-treated C2C12 myotube cells. GSK2656157, a selective first-in-class inhibitor of PERK, inhibited PERK activation in cells and suppressed tumor growth in a human tumor xenograft in mice (Su et al., 2013). 4μ8C is a highly selective and potent inhibitor of IRE1α splicing activity (Harrison et al., 2018). The CRISPR/Cas9 system has been used for genome editing purposes by numerous research groups (Adli, 2018; Nishizawa et al., 2004). In this study, inhibition of PERK, IRE1 and ATF6 by using GSK2656157, 4μ8C, each sh-RNA or CRISPR/Cas9 genome editing technology showed that changes in musclin expression is mediated by these three pathways. The bioinformatics prediction in our recent study showed the transcription factor ATF4, which is at downstream of PERK, may directly binding to the musclin promoter, and thus up-regulate the gene expression of musclin. This will be validated in our further study.

Musclin expression is augmented in the skeletal muscle of obese insulin resistant mice (Nishizawa et al., 2004). In addition, musclin inhibited insulin-stimulated glucose uptake and glycogen synthesis in myocytes (Chen et al., 2017; Nishizawa et al., 2004). The mechanism remain largely unknown. Akt is the serine/threonine kinase in the insulin signaling cascade (Manning and Toker, 2017). Normally, when the insulin receptor receives an insulin signal, insulin stimulated phosphorylation of Akt. The impairment in the phosphorylation of Akt leads to IR and reduced in glucose uptake (Kubota et al., 2018; Manning and Toker, 2017). This study found that silencing of the expression of musclin effectively relieved GlcN-induced dephosphorylation of Akt, indicating that GlcN induced IR at least partially through musclin. Besides, silencing of the expression of musclin effectively relieved GlcN-reduced glucose uptake and glycogen synthesis. Therefore, musclin could exert effects on glucose homeostasis that may be mediated via changes in the insulin sensitivity of skeletal muscle.

Furthermore, other report also showed that pre incubating muscles with musclin reduced Akt activation in the insulin-signaling cascade (Liu et al., 2008). Therefore, musclin has the autocrine effect in muscle cells. The paracrine effect of musclin in other tissues, such as liver or adipose tissue, remains unclear. Li et al. reported that the increased and decreased tendency of systolic blood pressure were observed in musclin transgenic mice and null mice respectively (Li et al., 2013). Conceivably, musclin may transmit important signal(s) to the skeletal muscle itself or to remote organs.

5. Conclusion

In summary, this study confirmed that GlcN induced ER stress and thus induced IR, resulting in increased plasma glucose levels in mice. GlcN caused an increase in musclin gene expression through UPR (PERK/IRE1/ATF6)s, representing an important factor responsible for IR induction in mice. The present findings indicate that excessive GlcN intake may have a toxicological effect on glucose metabolism in humans.

Acknowledgement

This work was supported by funds of the National Natural Science Foundation of China (Grant No. 21677044), the Open Project of State Key Laboratory of Urban Water Resource and Environment of Harbin Institute of Technology (Grant No. HCK201805), the National Funds for Creative Research Group of China (Grant No. 51121062), the Fundamental Research Funds for the Central Universities (Grant No. HIT. NSRIF. 201669).

Transparency document

Transparency document related to this article can be found online at https://doi.org/10.1016/j.fct.2018.12.051.

References

Adli, M., 2018. The CRISPR tool kit for genome editing and beyond. Nat. Commun. 9, 1911.
Anderson, J.W., Nicolosi, R.J., Borzelleca, J.F., 2005. Glucosamine effects in humans: a review of effects on glucose metabolism, side effects, safety considerations and efficacy. Food Chem. Toxicol. 43, 187–201.
Bettigole, S.E., Glimcher, L.H., 2015. Endoplasmic reticulum stress in immunity. Annu. Rev. Immunol. 33, 107–138.
Biazi, B.I., Zanetti, T.A., Baranoski, A., Corveloni, A.C., Mantovani, M.S., 2017. Cis-nerolidol induces endoplasmic reticulum stress and cell death in human hepatocellular carcinoma cells through extensive CYP2C19 and CYP1A2 oxidation. Basic Clin. Pharmacol. Toxicol. 121, 334–341.
Bohnert, K.R., McMillan, J.D., Kumar, A., 2018. Emerging roles of ER stress and unfolded protein response pathways in skeletal muscle health and disease. J. Cell. Physiol. 233, 67–78.
Chen, W.J., Liu, Y., Sui, Y.B., Zhang, B., Zhang, X.H., Yin, X.H., 2017. Increased circulating levels of musclin in newly diagnosed type 2 diabetic patients. Diabetes Vasc. Dis. Res. 14, 116–121.
Cubillos-Ruiz, J.R., Bettigole, S.E., Glimcher, L.H., 2017. Tumorigenic and immunosuppressive effects of endoplasmic reticulum stress in cancer. Cell 168, 692–706.
Dalirfardouei, R., Karimi, G., Jamialahmadi, K., 2016. Molecular mechanisms and biomedical applications of glucosamine as a potential multifunctional therapeutic agent. Life Sci. 152, 21–29.
Gu, N., Guo, Q., Mao, K., Hu, H., Jin, S., Zhou, Y., He, H., Oh, Y., Liu, C., Wu, Q., 2015. Palmitate increases musclin gene expression through activation of PERK signaling pathway in C2C12 myotubes. Biochem. Biophys. Res. Commun. 467, 521–526.
Harrison, S.R., Scambler, T., Oubussad, L., Wong, C., Wittmann, M., McDermott, M.F., Savic, S., 2018. Inositol-requiring enzyme 1-mediated downregulation of MicroRNA (miR)-146a and miR-155 in primary dermal fibroblasts across three TNFRSF1A mutations results in hyperresponsiveness to lipopolysaccharide. Front. Immunol. 9, 173.
Jeremic, N., Chaturvedi, P., Tyagi, S.C., 2017. Browning of white fat: novel insight into factors, mechanisms, and therapeutics. J. Cell. Physiol. 232, 61–68.
Kim, S.R., Kim, D.I., Kang, M.R., Lee, K.S., Park, S.Y., Jeong, J.S., Lee, Y.C., 2013. Endoplasmic reticulum stress influences bronchial asthma pathogenesis by modulating nuclear factor κB activation. J. Allergy Clin. Immunol. 132, 1397–1408.
Kong, C.S., Kim, J.A., Kim, S.K., 2009. Anti-obesity effect of sulfated glucosamine by AMPK signal pathway in 3T3-L1 adipocytes. Food Chem. Toxicol. 47, 2401–2406.
Kubota, T., Inoue, M., Kubota, N., Takamoto, I., Mineyama, T., Iwayama, K., Tokuyama, K., Moroi, M., Ueki, K., Yamauchi, T., Kadowaki, T., 2018. Downregulation of macrophage Irs2 by hyperinsulinemia impairs IL-4-indeuced M2a-subtype macrophage activation in obesity. Nat. Commun. 9, 4863.
Li, Y.X., Cheng, K.C., Asakawa, A., Kato, I., Sato, Y., Amitani, H., Kawamura, N., Cheng, J.T., Inui, A., 2013. Role of musclin in the pathogenesis of hypertension in rat. PLoS One 8, e72004.
Liong, S., Lappas, M., 2016. Endoplasmic reticulum stress regulates inflammation and insulin resistance in skeletal muscle from pregnant women. Mol. Cell. Endocrinol. 425, 11–25.
Liu, C.M., Ma, J.Q., Sun, J.M., Feng, Z.J., Cheng, C., Yang, W., Jiang, H., 2017. Association of changes in ER stress-mediated signaling pathway with lead-induced insulin resistance and apoptosis in rats and their prevention by A-type dimeric epigallocatechin-3-gallate. Food Chem. Toxicol. 110, 325–332.
Liu, Y., Huo, X., Pang, X.F., Zong, Z.H., Meng, X., Liu, G.L., 2008. Musclin inhibits insulin actication of Akt/protein Kinase B in rat skeletal muscle. J. Int. Med. Res. 36, 496–504.
Longo, M., Spinellim, R., D'Esposito, V., Zatterale, F., Fiory, F., Nigro, C., Raciti, G.A., Miele, C., Formisano, P., Beguinot, F., Di, J.B., 2016. Pathologic endoplasmic reticulum stress induced by glucotoxic insults inhibits adipocyte differentiation and induces an inflammatory phenotype. Biochim. Biophys. Acta 1863, 1146–1156.
Malhi, H., Kaufman, R.J., 2011. Endoplasmic reticulum stress in liver disease. J. Hepatol. 54, 795–809.
Manning, B.D., Toker, A., 2017. AKT/PKB signaling: navigating the network. Cell 169, 381–405.
Naito, Y., Hino, K., Bono, H., Ui-Tei, K., 2015. CRISPRdirect: software for designing CRISPR/Cas guide RNA with reduced off-target sites. Bioinformatics 31, 1120–1123.
Nishizawa, H., Matsuda, M., Yamada, Y., Kawai, K., Suzuki, E., Makishima, M., Kitamura, T., Shimomura, I., 2004. Musclin, a novel skeletal muscle-derived secretory factor. J. Biol. Chem. 279 19391e19395.
Park, E., Yu, K.H., Kim, D.K., Kim, S., Sapkota, K., Kim, S.J., Kim, C.S., Chun, H.S., 2014. Protective effects of N-acetylcysteine against monosodium glutamate-induced astrocytic cell death. Food Chem. Toxicol. 67, 1–9.
Pedersen, B.,K., Febbraio, M.A., 2008. Muscle as an endocrine organ: focus on musclederived interleukin-6. Physiol. Rev. 88, 1379e1406.
Plomgaard, P., Nielsen, A.R., Fischer, C.P., Mortensen, O.H., Broholm, C., Penkowa, M., Krogh-Madsen, R., Erikstrup, C., Lindegaard, B., Petersen, A.M., Taudorf, S., Pedersen, B.K., 2007. Associations between insulin resistance and TNF alpha in plasma, skeletal muscle and adipose tissue in humans with and without type 2 diabetes. Diabetologia 50, 2562e2571.
Reginster, J.Y., Neuprez, A., Lecart, M.P., Sarlet, N., Bruyere, O., 2012. Role of glucosamine in the treatment for osteoarthritis. Rheumatol. Int. 32, 2959–2967.
Rozpedek, W., Pytel, D., Mucha, B., Leszczynska, H., Diehl, J.A., Majsterek, I., 2016. The role of the PERK/eIF2α/ATF4/CHOP signaling pathway in tumor progression during endoplasmic reticulum stress. Curr. Mol. Med. 16, 533–544.
Simon, R.R., Marks, V., Leeds, A.R., Anderson, J.W., 2011. A comprehensive review of oral glucosamine use and effects on glucose metabolism in normal and diabetic individuals. Diabetes Metab. Res. Rev. 27, 14–27.
Su, L., Chen, X., Wu, J., Lin, B., Zhang, H., Lan, L., Luo, H., 2013. Galangin inhibits proliferation of hepatocellular carcinoma cells by inducing endoplasmic reticulum stress. Food Chem. Toxicol. 62, 810–816.
Takahashi, N., Kimura, A.P., Naito, S., Yoshida, M., Kumano, O., Suzuki, T., Itaya, S., Moriya, M., Tsuji, M., Ieko, M., 2017. Sarcolipin expression is repressed by endoplasmic reticulum stress in C2C12 myotubes. J. Physiol. Biochem. 73, 531–538.
van der Harg, J.M., van Heest, J.C., Bangel, F.N., Patiwael, S., van Weering, J.R., Scheper, W., 2017. The UPR reduces glucose metabolism via IRE1 signaling. Biochim. Biophys. Acta 1864, 655–665.
Wu, W., Yao, X., Jiang, L., Zhang, Q., Bai, J., Qiu, T., Yang, L., Gao, N., Yang, G., Liu, X., Chen, M., Sun, X., 2018. Pancreatic islet-autonomous effect of arsenic on insulin secretion through endoplasmic reticulum stress-autophagy pathway. Food Chem. Toxicol. 111, 19–26.